



# ***NON LINEAR SHOCK ACCELERATION AND $\gamma$ -RAY EMISSION FROM TYCHO AND KEPLER***



***Giovanni Morlino***

***INAF/Osservatorio Astrofisico di Arcetri***

**In collaboration with: Damiano Caprioli**

**GAMMA 2012**

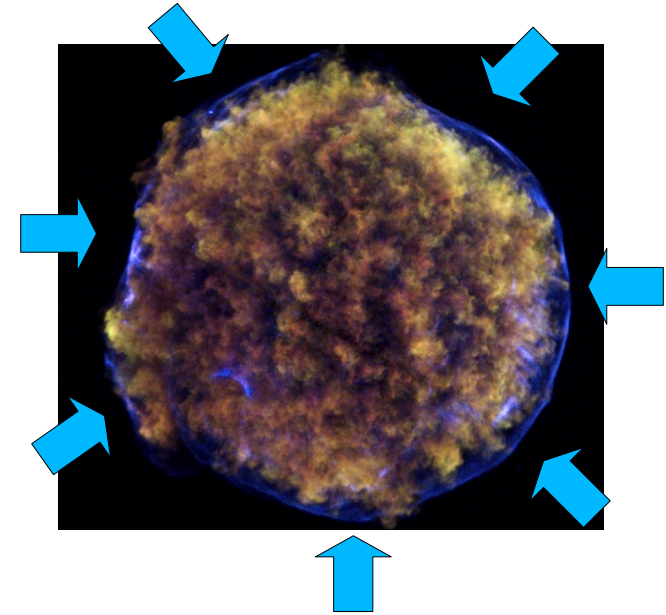
**Heidelberg, July 9<sup>th</sup> – 13<sup>th</sup>, 2012**

# Hints of efficient acceleration in Tycho

Tycho's SNR presents several hints of efficient hadronic acceleration:

1) Thin non-thermal X-ray filaments → **evidence for magnetic field amplification ( $B \sim 200\text{-}300 \mu\text{G}$ )**

[Hwang et al(2002); Bamba et al (2005)]



# Hints of efficient acceleration in Tycho

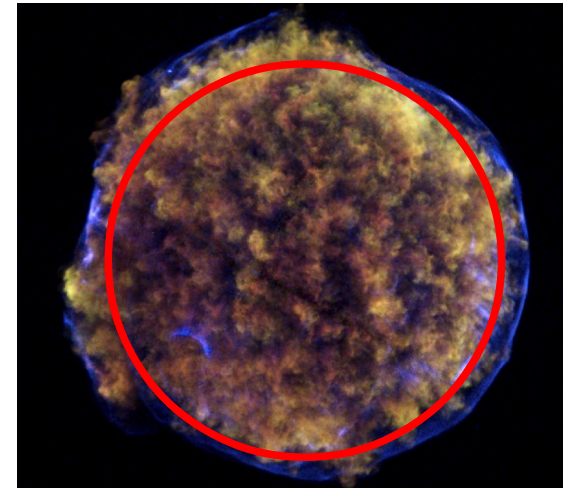
Tycho's SNR presents several hints of efficient hadronic acceleration:

1) Thin non-thermal X-ray filaments → **evidence for magnetic field amplification ( $B \sim 200\text{-}300 \mu\text{G}$ )**

[Hwang et al (2002); Bamba et al (2005)]

2) Small distance between CD and FS → **downstream plasma should be more compressible than standard hydrodynamical prediction (as predicted by efficient particle acceleration)**

[Warren et al. (2005)]





# Hints of efficient acceleration in Tycho

Tycho's SNR presents several hints of efficient hadronic acceleration:

1) Thin non-thermal X-ray filaments → **evidence for magnetic field amplification ( $B \sim 200\text{-}300 \mu\text{G}$ )**

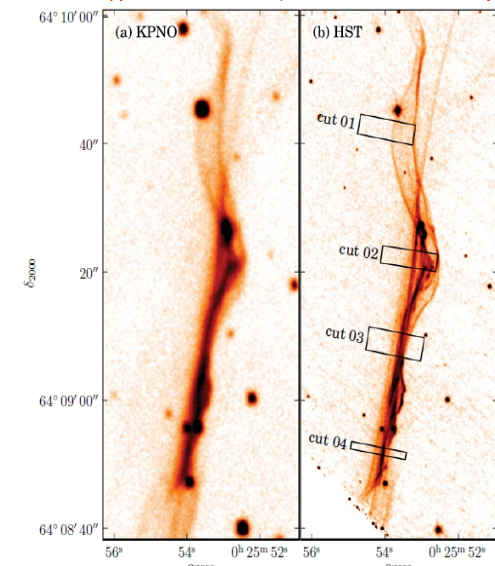
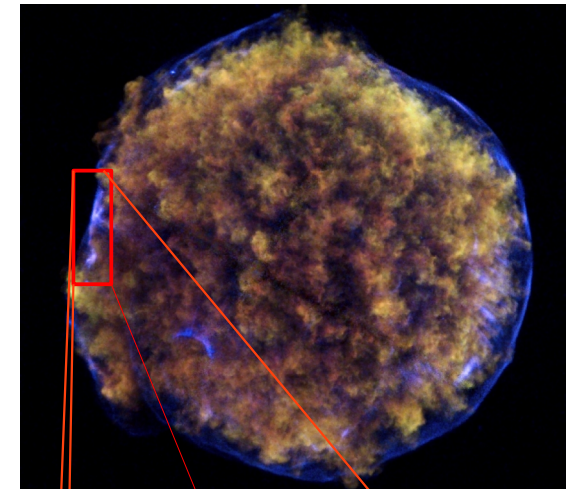
[Hwang et al (2002); Bamba et al (2005)]

2) Small distance between CD and FS → **downstream plasma should be more compressible than standard hydrodynamical prediction (as predicted by efficient particle acceleration)**

[Warren et al. (2005)]

3) Detection of Balmer lines in the region ahead of the shock → **has been interpreted as neutral hydrogen heated in the CR-induced precursor**

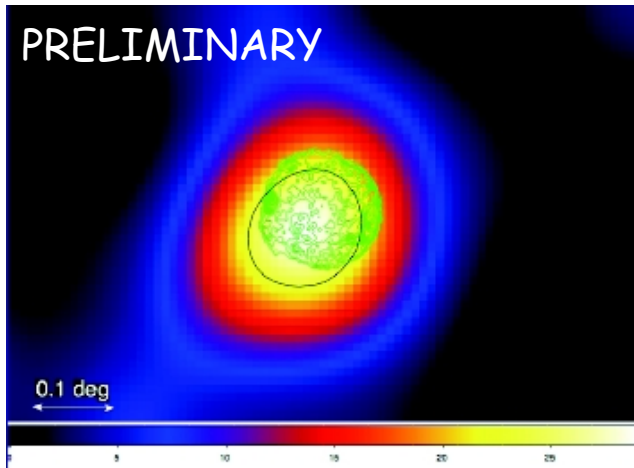
[Lee et al. (2010)]



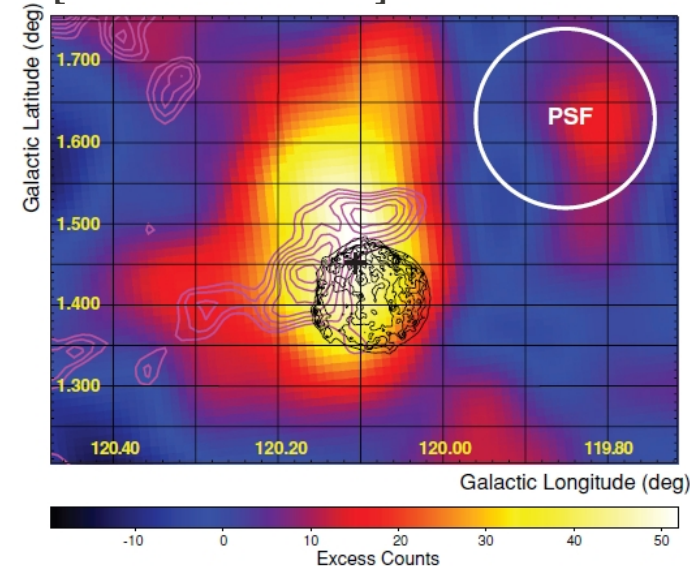
Hubble space telescope

# Tycho detection in gamma emission

Fermi TS map 1-100 GeV  
[Giordano et al. 2011]



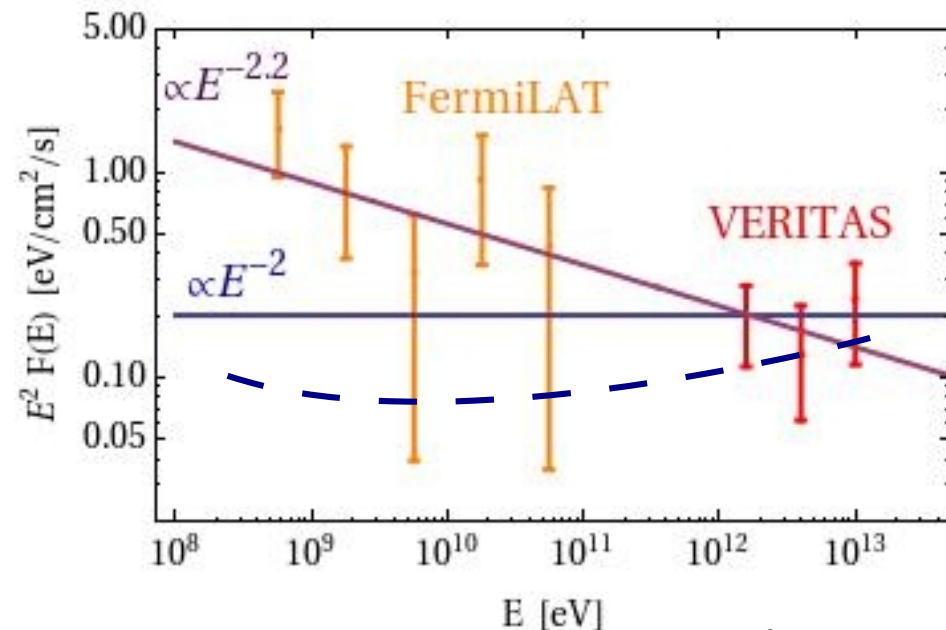
VERITAS map  $E > 1$  TeV  
[Acciari et al. 2011]



Measured spectral slope in gamma-rays:

FermiLAT  $\Gamma = 2.3 \pm 0.1$  [Giodano et al. 2011]

VERITAS  $\Gamma = 1.95 \pm 0.51_{\text{stat}} \pm 0.30_{\text{sys}}$  [Acciari et al. 2011]



— Linear theory  $\rightarrow f_p(E) \propto E^{-2} \Rightarrow F(\pi_0 \rightarrow \gamma\gamma) \propto E^{-2}$

- - Non-linear theory  $\rightarrow f_p(E) \propto E^{-\Gamma}, \Gamma > 2$

**Is it possible to explain the  $\gamma$ -ray spectrum and at the same time all the other spectral and morphological properties?**

# Description of the model: remnant evolution

## Type Ia SN

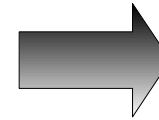
Detected echo light  
(Krause et al., 2008)

$$\begin{aligned}E_{SN} &= 10^{51} \text{ erg} \\M_{eje} &= 1 M_{sol} \\T_{SNR} &= 439 \text{ yr} \\f(v) &\propto (v/v_{eje})^{-7}\end{aligned}$$

## Expansion in homogeneous ISM

No evidences of interaction between  
the shock and a molecular clouds  
[Tian & Leahy (2011)]

$$\begin{aligned}n_0 &= 0.3 \text{ proton/cm}^3 \quad (\text{free parameter}) \\T_0 &= 10^4 \text{ K}\end{aligned}$$



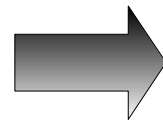
Tycho is at the end of  
the free expansion phase

$$T_{ST} = 463 \text{ yr} > T_{SNR}$$

## Analytic solution for ejecta dominated phase

[Truelove & McKee 1999]

$$\begin{aligned}R_{sh}(t) &= 4.06 \left( \frac{t}{T_{ST}} \right)^{4/7} \text{ pc} \\V_{sh}(t) &= 4875 \left( \frac{t}{T_{ST}} \right)^{-3/7} \text{ km/s}\end{aligned}$$



$$\begin{aligned}R_{sh}(T_{SNR}) &= 3.94 \text{ pc} \rightarrow d = 3.3 \text{ kpc} \\V_{sh}(T_{SNR}) &= 4990 \text{ km/s}\end{aligned}$$

Compatible with all  
existing estimates

# Description of the model: particle acceleration

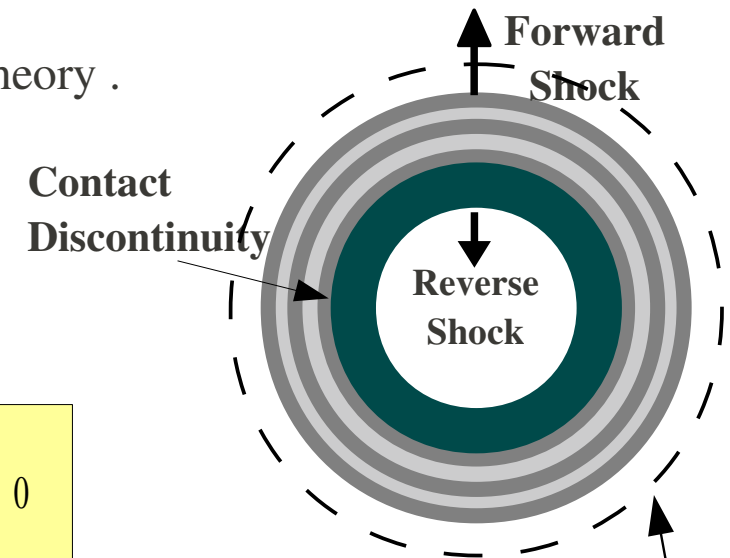
We couple the remnant evolution to the stationary Shock Acceleration (NLDSA)

The remnant evolution is divided in several time steps  $\Delta t$ .

For each time step we apply the stationary shock acceleration theory .

Particle acceleration: we adopt the semi-analytical framework from Amato & Blasi (2006) and Caprioli et al. (2010)

$$\frac{d f_{CR}(x, p)}{dt} = \frac{\partial f_{CR}}{\partial t} - u(x) \frac{\partial f_{CR}}{\partial x} = \frac{\partial}{\partial x} \left[ D(x, p) \frac{\partial f_{CR}}{\partial x} \right] + \frac{1}{3} \frac{du(x)}{dx} p \frac{\partial f_{CR}}{\partial p} + Q(x, p) \equiv 0$$



- Diffusion: Accelerated particles diffuse with Bohm-like diffusion coefficient in the self-generate magnetic turbulence via **resonant streaming instability**
- Escape boundary: particles escape from the accelerator if they reach a distance  $d \sim \chi_{\text{esc}} R_{\text{SNR}}$  with  $\chi_{\text{esc}} \sim 10\% \rightarrow$  this fix the maximum energy.

# Magnetic field amplification and damping

**UPSTREAM:** transport of magnetic turbulence with growth due to resonant amplification

$$\frac{dF_w}{dx} = u(x) \frac{dP_w}{dx} + v_A \frac{dP_{cr}}{dx} \rightarrow P_w(x) = \frac{B_1(x)^2}{8\pi\rho_0 V_{sh}} \simeq \frac{1+U(x)}{4M_A(x)U(x)} P_{cr}(x)$$

**DOWNSTREAM:** transport with adiabatic losses and damping

Non-linear Landau damping  
(Ptuskin & Zirakashvili, 2003):

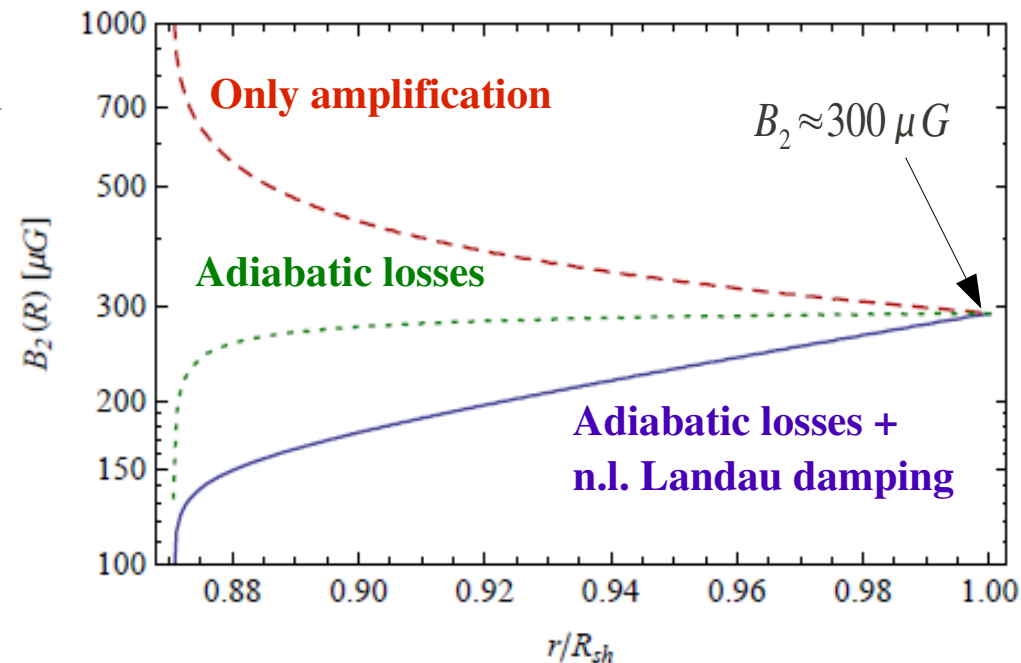
$$\Gamma_{nl} \simeq 0.05 k_{min} v_A \simeq 0.05 \frac{v_A}{r_L(p_{max})} \quad \text{Damping rate averaged on the different scales}$$

$$\lambda_{nl} \simeq \frac{u_2}{\Gamma_{nl}} \approx 3.5 pc \quad \text{Damping scale}$$

$$L(t_0, t) = [\rho(t)/\rho_0]^{1/3} \quad \text{Adiabatic losses}$$

$$B_2(x) = B_2(t_0) L(t_0, t)^2 \exp\left[-\frac{R_{sh}-x}{\lambda_{nl}}\right]$$

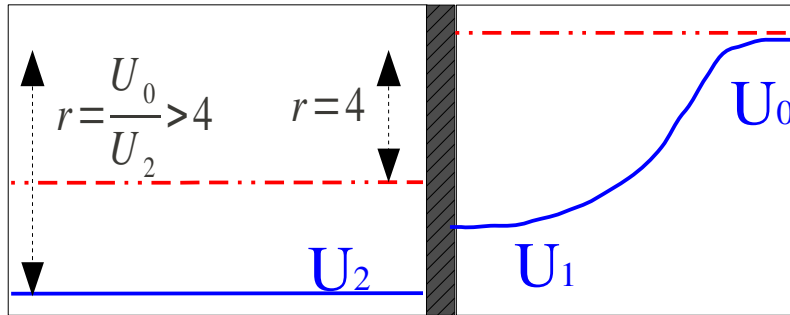
Downstream profile of magnetic field



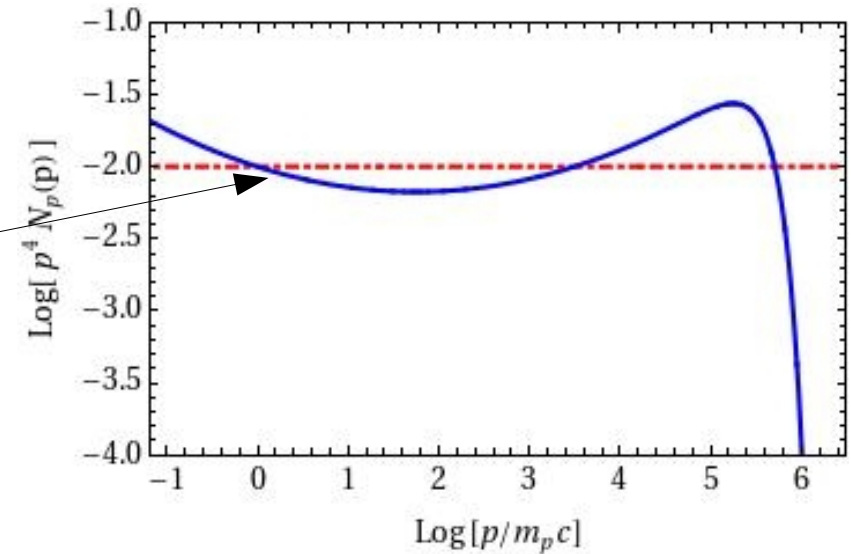


# The role of scattering centers in presence of strong magnetic amplification

In the standard NLDSA the CR pressure modifies the shock structure in such a way to produce concave particle spectra with spectral slope  $> 2$  at higher energies

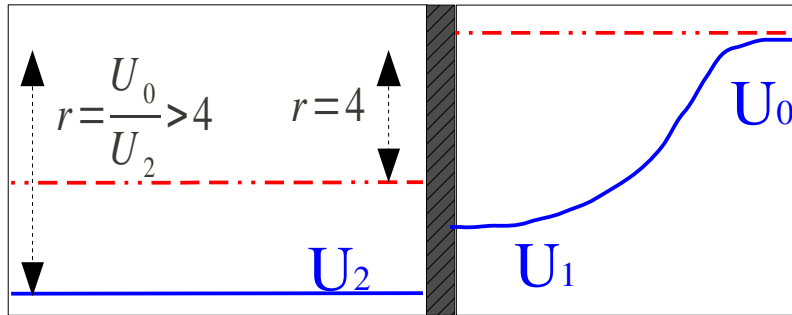


Shock  
modified  
by CRs

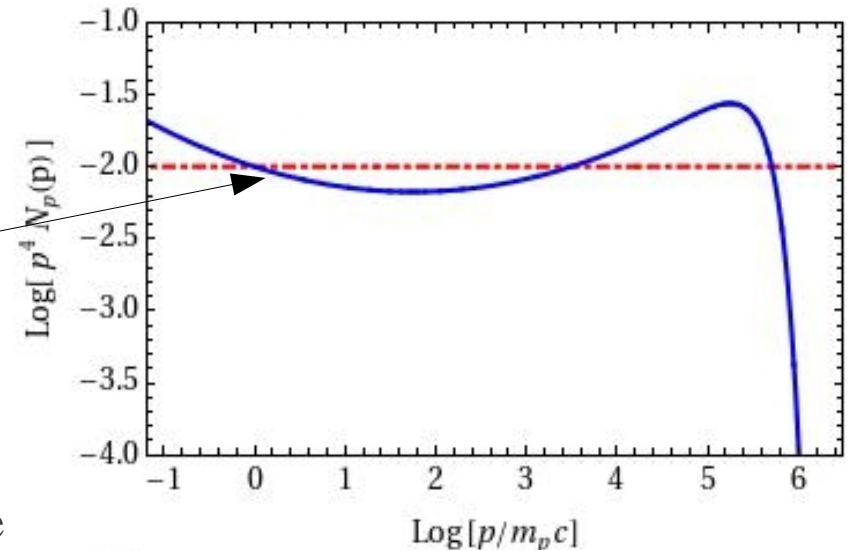


# The role of scattering centers in presence of strong magnetic amplification

In the standard NLDSA the CR pressure modifies the shock structure in such a way to produce concave particle spectra with spectral slope  $< 2$  at higher energies



Shock  
modified  
by CRs

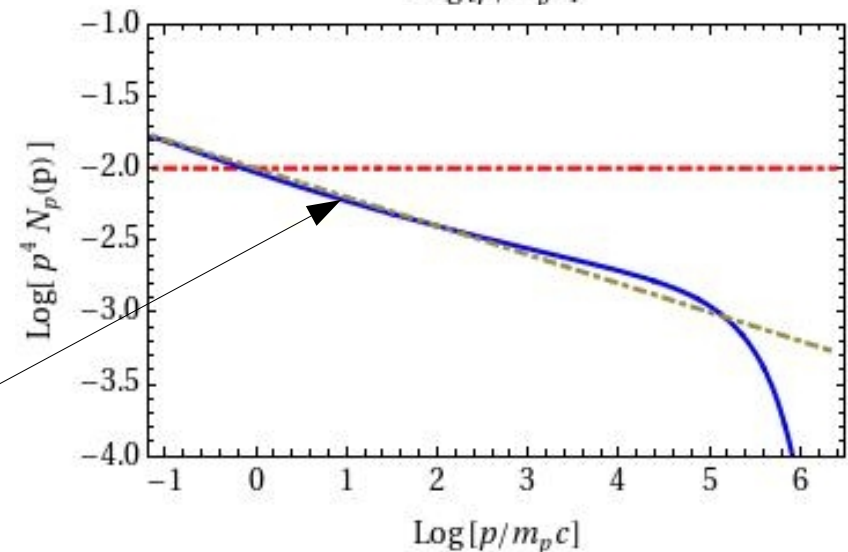


When the magnetic field is strongly amplified the Alfvén speed upstream can become a non negligible fraction of the shock speed. In this case the effective compression ratio is:

$$r = \frac{u_1 - v_{A,1}}{u_2 \pm v_{A,2}} \simeq \frac{u_1 - v_{A,1}}{u_2}$$

Downstream  $v_{A,2} \approx 0$  because of helicity mixing.  
In the case of Tycho:

$$v_{A,1} = \frac{B_1}{\sqrt{4\pi\rho_1}} \approx 0.15V_{sh} \rightarrow s = \frac{r+2}{r-1} \simeq 4.2 \quad (2.2 \text{ in energy})$$

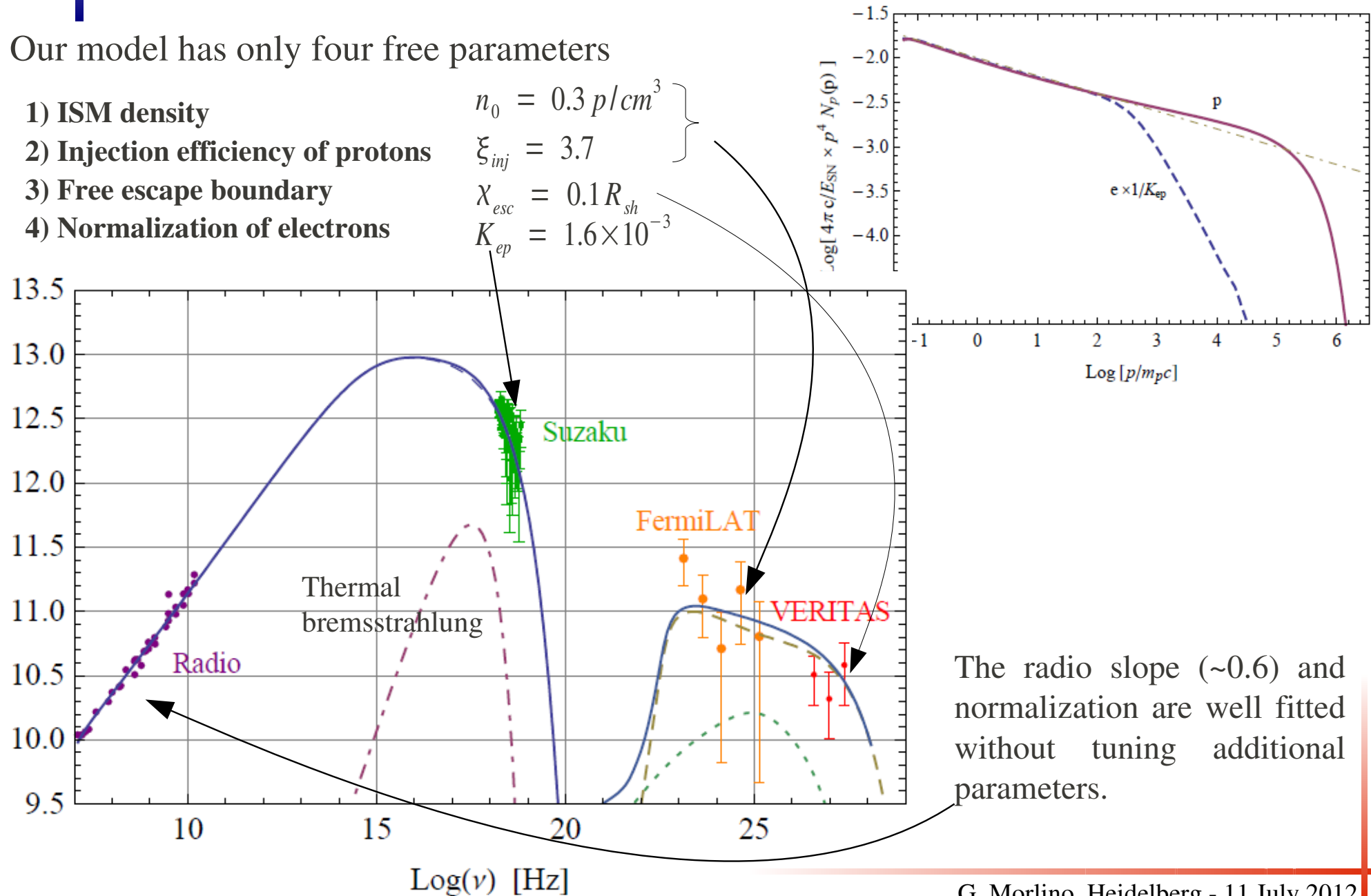


# Multi-wavelength spectrum

Our model has only four free parameters

- 1) ISM density
- 2) Injection efficiency of protons
- 3) Free escape boundary
- 4) Normalization of electrons

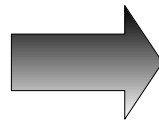
$$\left. \begin{aligned} n_0 &= 0.3 \text{ p/cm}^3 \\ \xi_{inj} &= 3.7 \\ \chi_{esc} &= 0.1 R_{sh} \\ K_{ep} &= 1.6 \times 10^{-3} \end{aligned} \right\}$$



The radio slope ( $\sim 0.6$ ) and normalization are well fitted without tuning additional parameters.

# Gamma spectrum

The dominant process in the GeV-TeV range is the pion decay produced in hadronic collisions



Maximum proton energy:

$$p_{max} = 470 \text{ TeV}/c$$

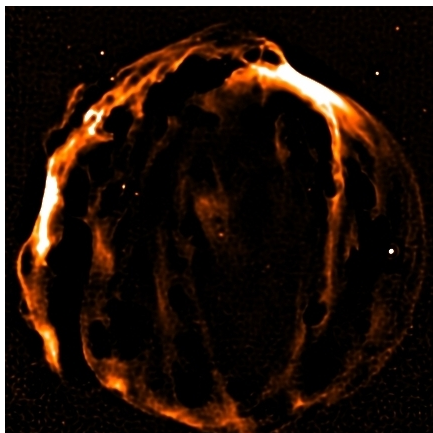
Kinetic energy converted into CRs :  $\epsilon_{CR} = 0.12$

## ELECTRONIC PROCESSES:

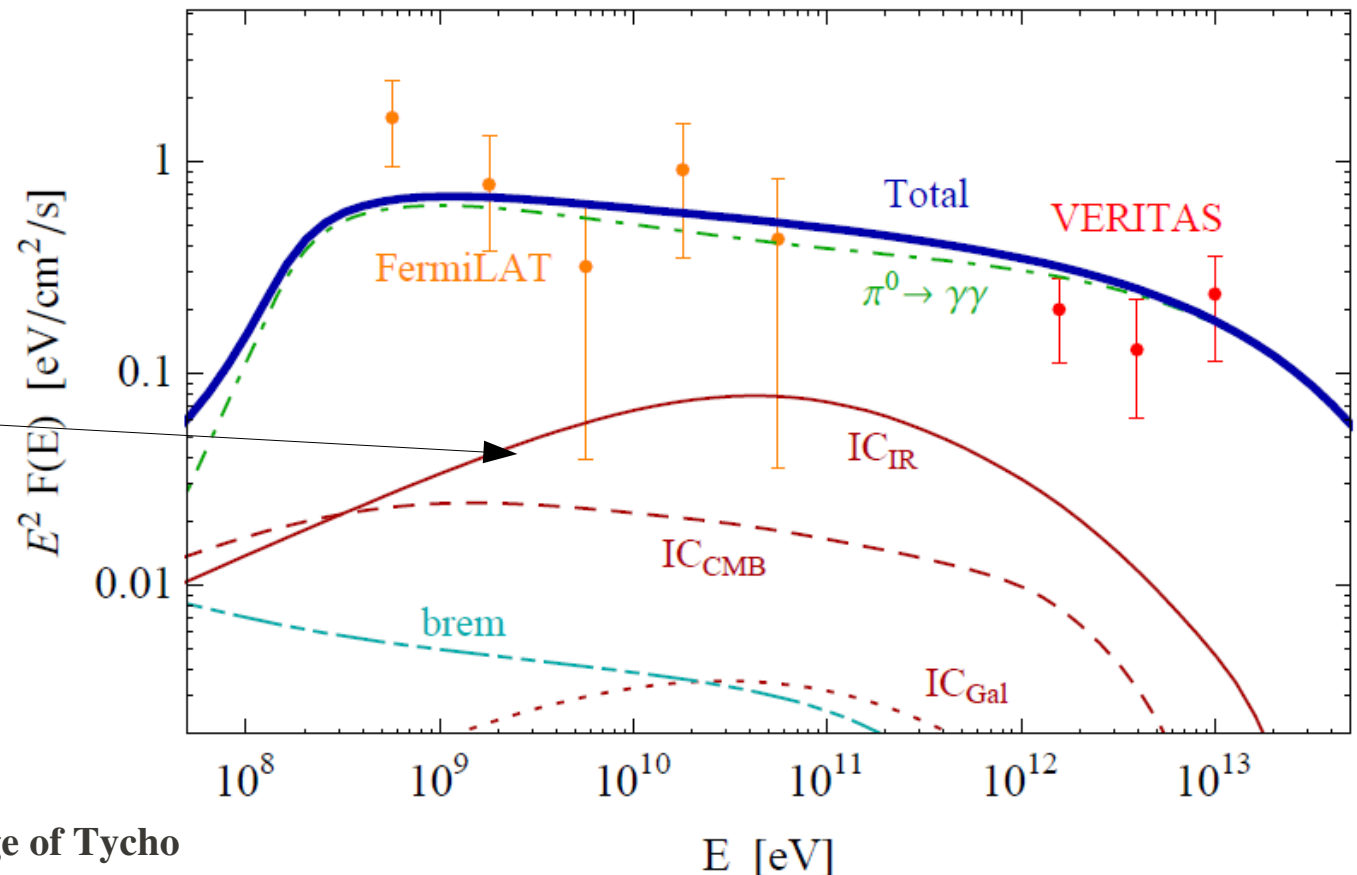
Non-thermal bremsstrahlung is totally negligible

Inverse Compton with:

- 1) CMB
- 2) Galactic light (opt+IR)
- 3) local dust-IR radiation



Spitzer image of Tycho  
at 24  $\mu\text{m}$

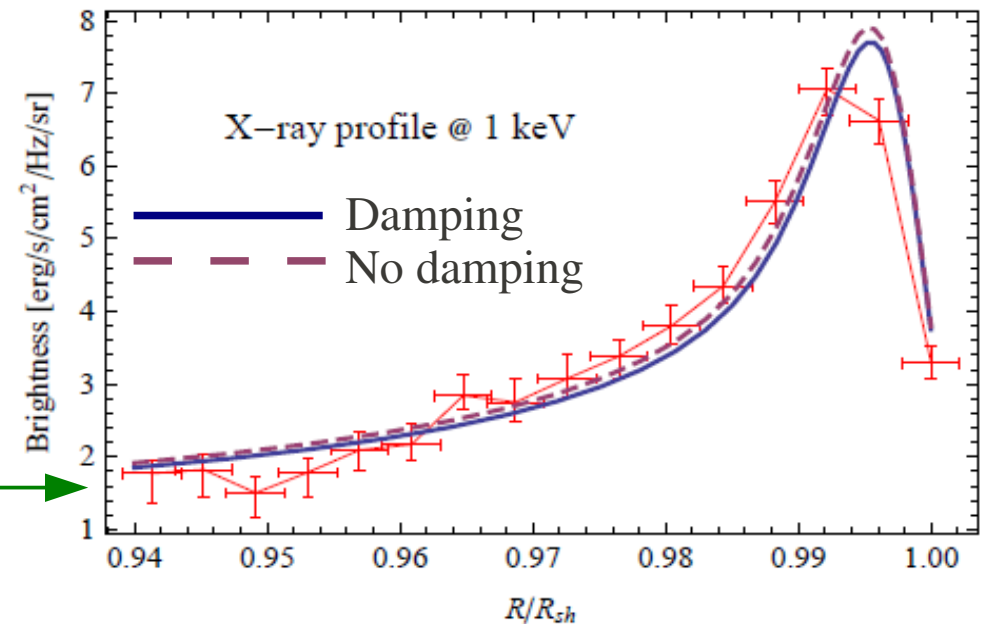
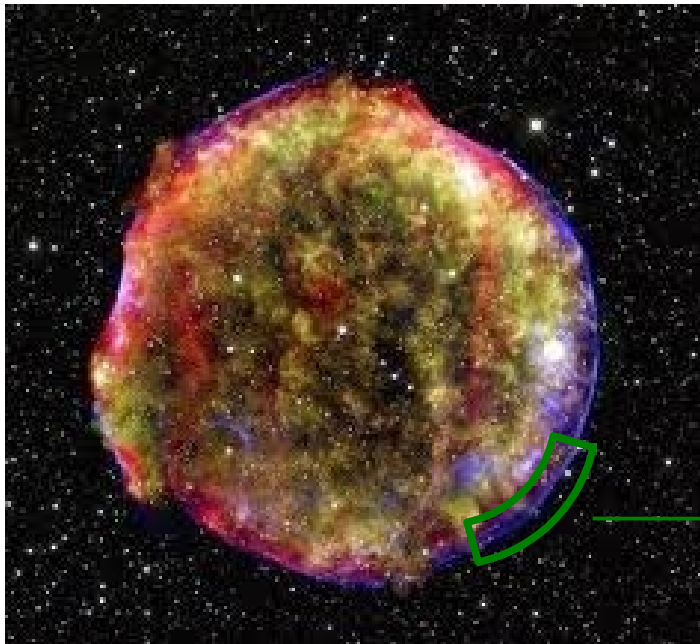




# Radial profile of X-ray emission

Filamentary structure of non-thermal X-ray emission is well reproduced

- The small filaments' thickness is a consequence of rapid synchrotron losses in a strong magnetic field ( $B_2 \approx 300 \mu\text{G}$ ).
- Non-linear Landau damping plays a minor role because the damping scale is large,  $\lambda \sim 3 \text{ pc}$ .

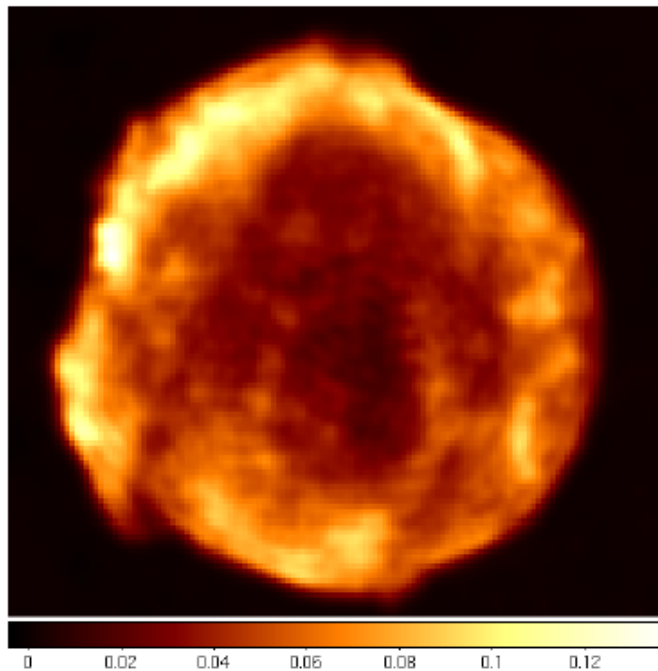


Chandra X-ray map.

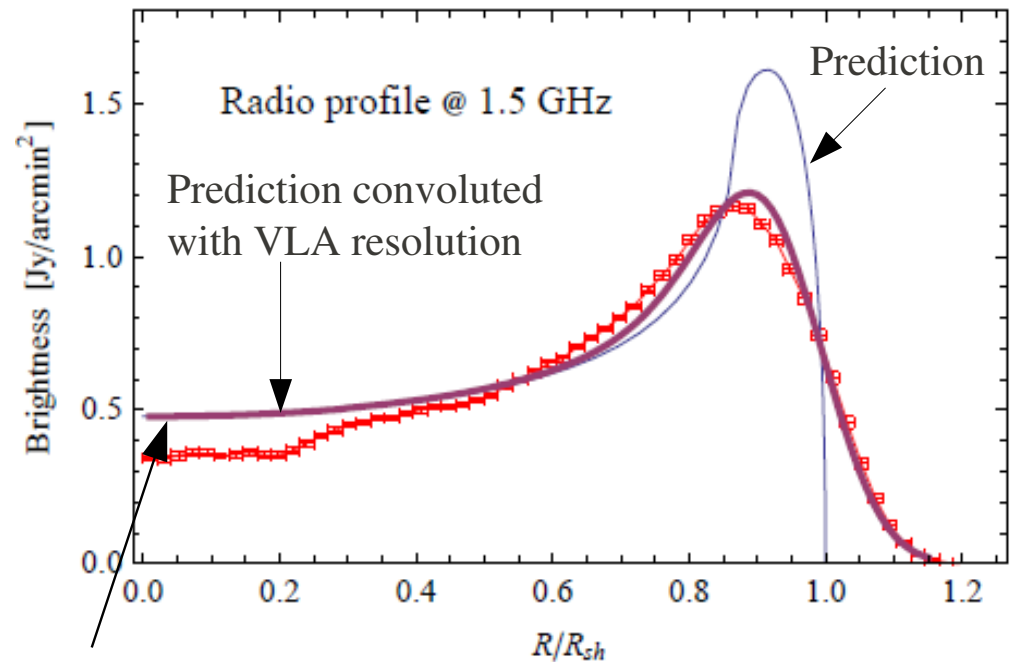
Data for the green sector are from  
Cassam-Chenaï et al (2007)

# Radial profile of radio emission

- Electron spectrum and magnetic field strength in the downstream well reproduce the morphology of radio synchrotron emission.
- For the radio emission we need the damping otherwise we over predict the flux by a factor  $\sim 5$



Radio map at 1.5 GHz from  
NRAO/VLA archive Survey



The excess in the inner part of the remnant could be due to small deviation from perfect spherical symmetry

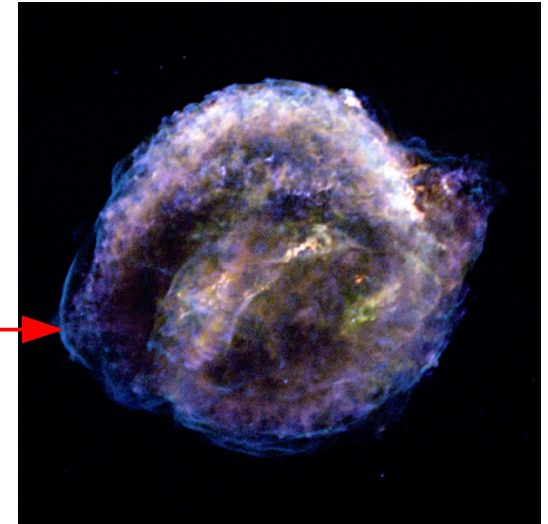
We find no evidence of efficient particle acceleration at the reverse shock

# Application to the Kepler's SNR

[D. Caprioli & G.M., preliminary results]

The Kepler's Remnant shows remarkable similarities with Tycho:

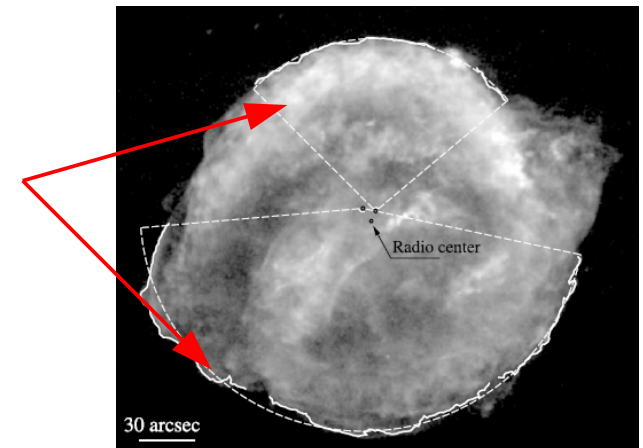
- both originate from Type Ia SN
- similar age (408 vs 440 yrs)
- similar radio spectral index (0.64 vs 0.65)
- presence of non-thermal X-ray emission in thin filaments



But also differences:

- Kepler is not detected in gamma rays (larger distance?)
- Several north-south asymmetry has been detected
  - Radio and X-ray emission more pronounced in the North
  - different shock speed
  - different expansion rate

Due to expansion in a non-uniform CSM  
(probably progenitor's wind?)



Chandra X-ray map.  
From Katsuda et al (2008)

**We apply a model similar to the one used for Tycho:  
results must be taken with care because we use uniform CSM  
density**

# Multi-wavelength spectrum of Kepler

[D. Caprioli & G.M., preliminary results]

## Assumed

$$\begin{aligned} E_{SN} &= 10^{51} \text{ erg} \\ M_{eje} &= 1 M_{sol} \\ T_{SNR} &= 400 \text{ yr} \\ f(\nu) &\propto (\nu/\nu_{eje})^{-7} \end{aligned}$$

## Fitted

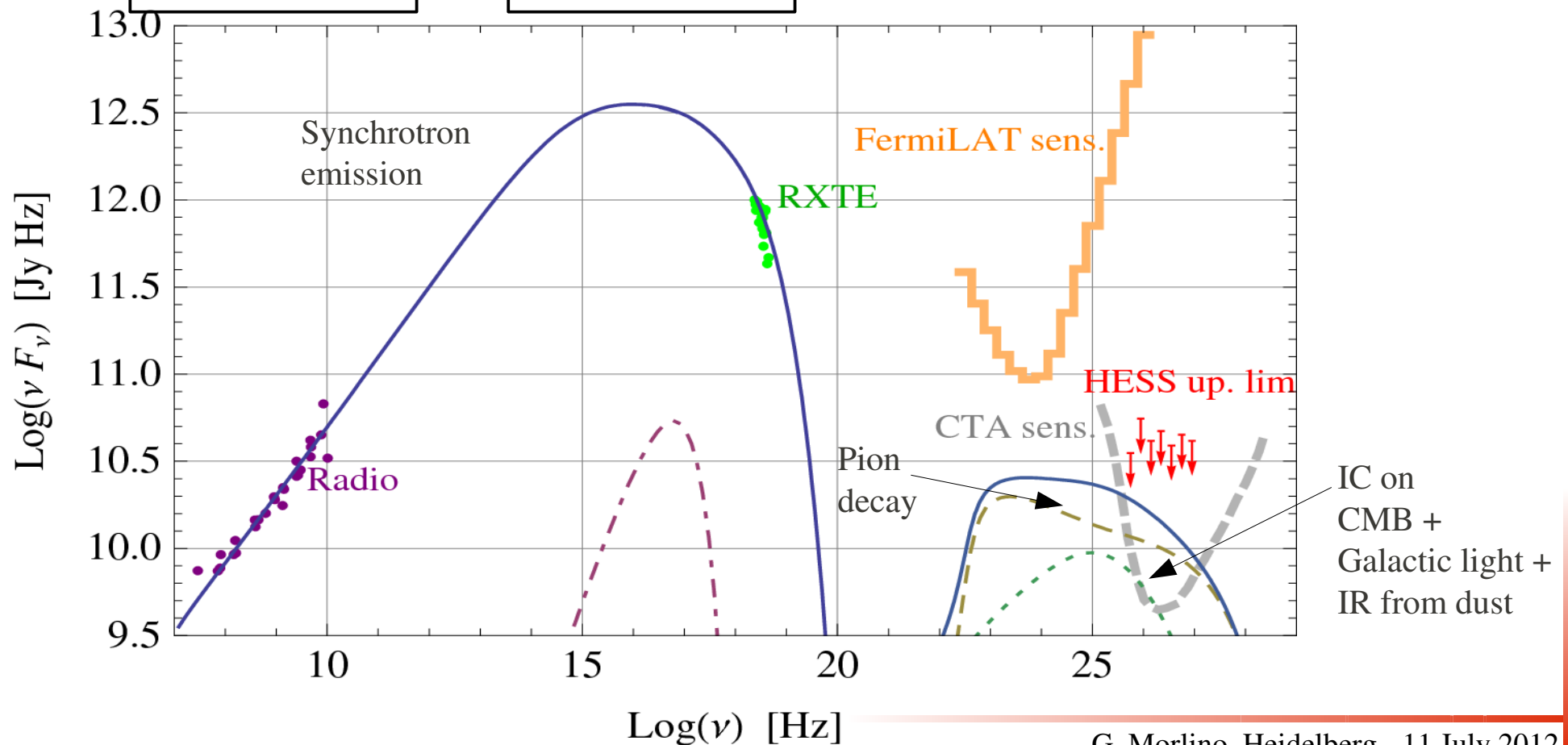
$$\begin{aligned} n_0 &= 0.3 \text{ p/cm}^3 \\ \xi_{inj} &= 3.7 \\ \chi_{esc} &= 0.1 R_{sh} \\ K_{ep} &= 2.8 \times 10^{-3} \end{aligned}$$

## Inferred

$$\begin{aligned} d &= 7.1 \text{ pc} \\ V_{sh} &= 5200 \text{ km/s} \\ R_{sh} &= 3.7 \text{ pc} \end{aligned}$$

## CR efficiency

$$\epsilon_{CR} \simeq 12\%$$

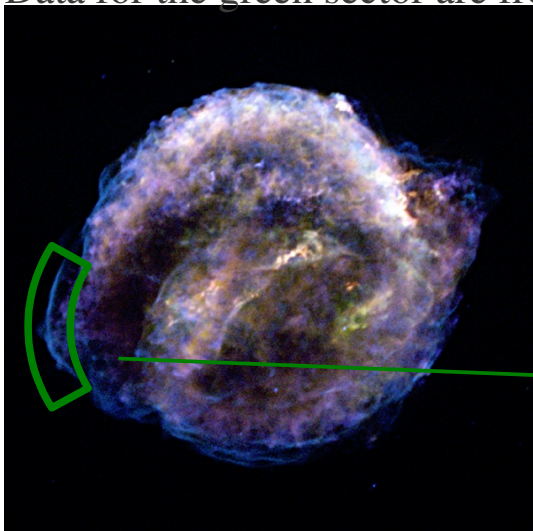




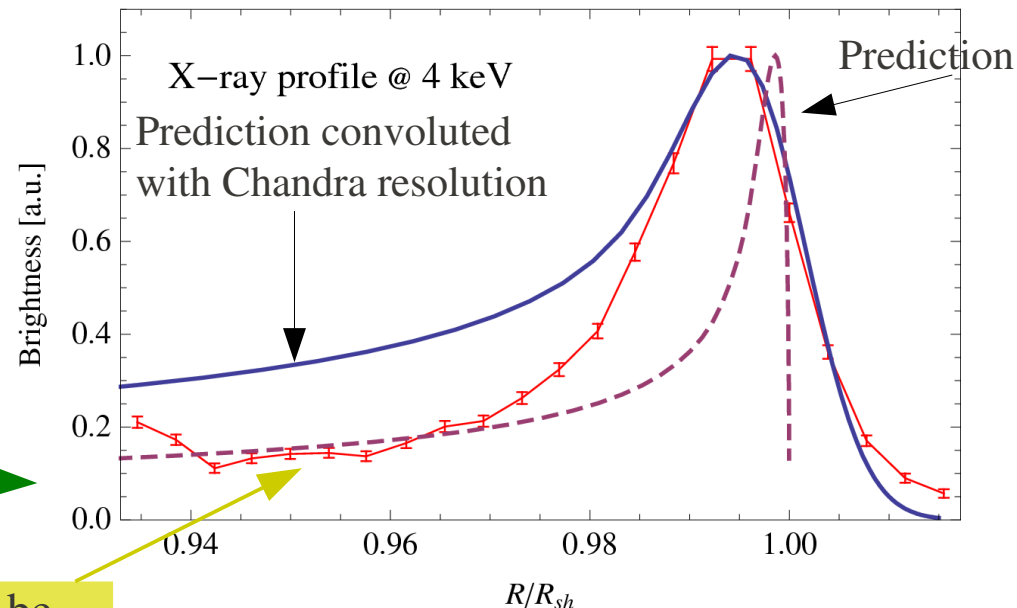
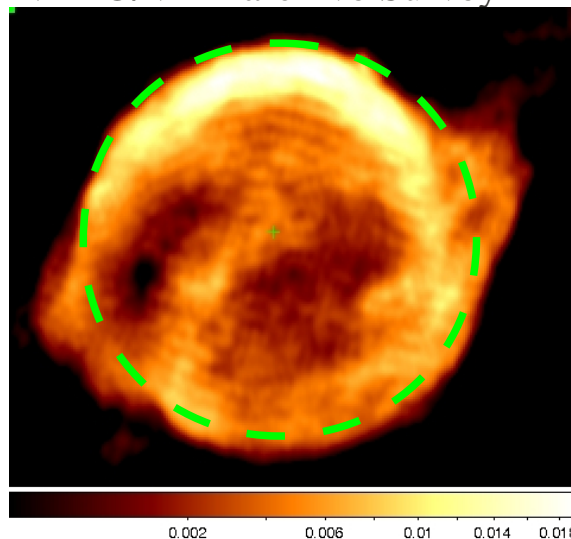
# Radial profile of X and radio emission for Kepler

Chandra X-ray map.

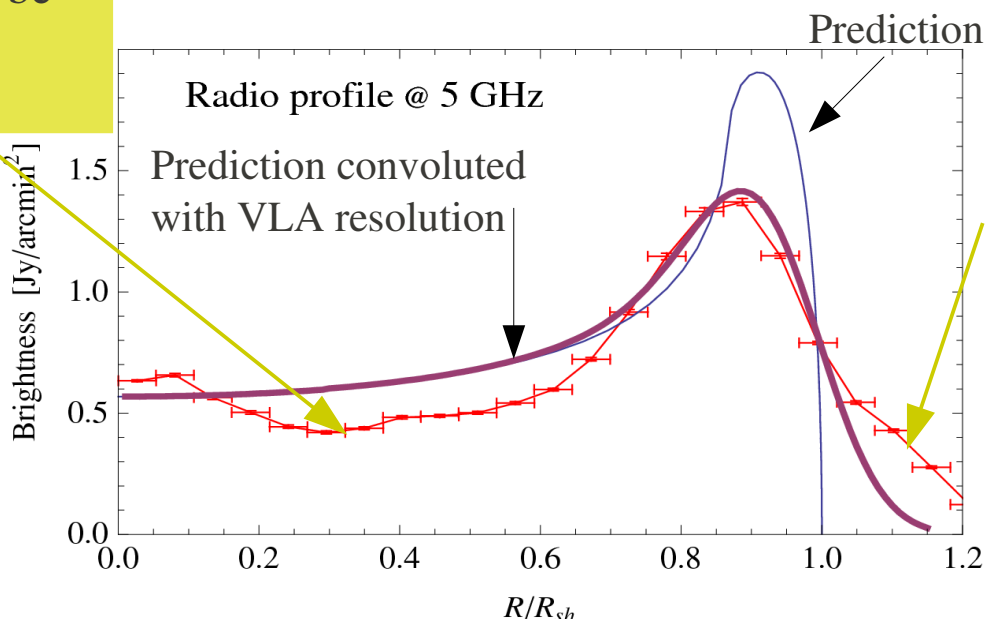
Data for the green sector are from Vink (2008)



Radio map at 5 GHz from NRAO/VLA archive Survey



These excesses could be due to deviation from spherical symmetry





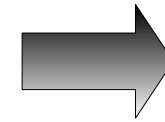
# Conclusions



Non thermal emission from the Tycho's SNR can be well accounted for by NLDSA:



- Flux and spectral shape of GeV-TeV emission
- Non-thermal X-ray emission
- Total flux and spectral index of radio emission
- Thickness of X-ray filaments
- Morphology of radio emission
- Distance between CD and FS




$$\begin{aligned} E_{\text{max}} \text{ (protons)} &\simeq 470 \text{ TeV} \\ \epsilon_{\text{CR}} &\simeq 12\% \end{aligned}$$

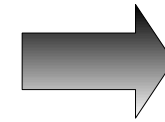
**We consider Tycho the first clear example of efficient CR accelerator**



# Conclusions

## Non thermal emission from the Tycho's SNR can be well accounted for by NLDSA:



- 
- Flux and spectral shape of GeV-TeV emission
  - Non-thermal X-ray emission
  - Total flux and spectral index of radio emission
  - Thickness of X-ray filaments
  - Morphology of radio emission
  - Distance between CD and FS



$$E_{\max} \text{ (protons)} \simeq 470 \text{ TeV}$$
$$\epsilon_{\text{CR}} \simeq 12\%$$

**We consider Tycho the first clear example of efficient CR accelerator**

## Application to Kepler:

- 
- Non-thermal X-ray emission
  - Total flux and spectral index of radio emission
- 
- Thickness of X-ray filaments
  - Morphology of radio emission




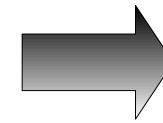
**Non uniform CSM**



# Conclusions

## Non thermal emission from the Tycho's SNR can be well accounted for by NLDSA:



- 
- Flux and spectral shape of GeV-TeV emission
  - Non-thermal X-ray emission
  - Total flux and spectral index of radio emission
  - Thickness of X-ray filaments
  - Morphology of radio emission
  - Distance between CD and FS



$$\begin{aligned} E_{\max} \text{ (protons)} &\simeq 470 \text{ TeV} \\ \epsilon_{\text{CR}} &\simeq 12\% \end{aligned}$$

**We consider Tycho the first clear example of efficient CR accelerator**

## Application to Kepler:

- 
- Non-thermal X-ray emission
  - Total flux and spectral index of radio emission
- 
- Thickness of X-ray filaments
  - Morphology of radio emission

← **Non uniform CSM**

**1) A crucial role is played by the modified speed of scattering centers induced by magnetic amplification. If this effects does not occurs, NLDSA cannot explain the observed spectrum**  
→ other mechanism should be invoked to steepen the particle spectrum

**2) We are unable to explain gamma-ray emission using leptonic processes only and simultaneously account for observations in other wavelengths**



# Electron spectrum

## Electron spectrum at the shock position

from Zirakashvily & Aharonian (2007)

$$f_{e,0}(p) = K_{ep} \times f_{p,0}(p) \left[ 1 + 0.523 \left( p/p_{e,max} \right)^{9/4} \right]^2 \exp \left[ -p^2/p_{e,max}^2 \right]$$

The maximum energy is determined by synchrotron losses which produces a quadratic exponential cut-off

$$\tau_{loss}(p_{max}, B) = t_{acc}(p_{max}, B)$$

## Evolution of electron energy downstream of the shock

from Reynolds (1988)

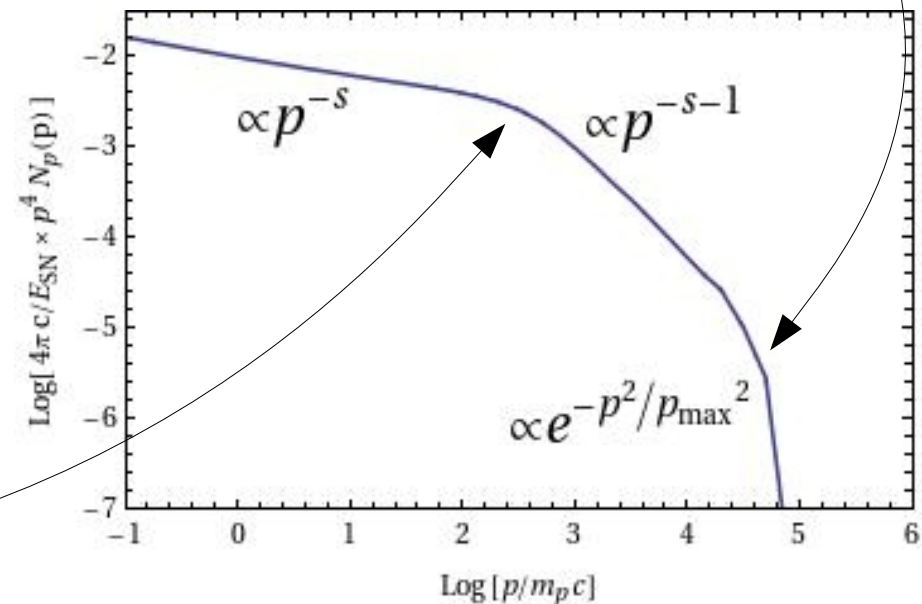
$$\frac{dE}{dt} = -\frac{4}{3} \sigma_T \left( \frac{E}{m_e c^2} \right)^2 \frac{B_{eff}^2}{8\pi} - \frac{E}{L} \frac{dL}{dt}$$

Synchrotron +  
Inverse Compton losses

Adiabatic losses

Synchrotron losses downstream determines a slope change for  $p > p_{roll}$

$$\tau_{loss}(p_{roll}, B_2) = T_{SNR}$$



# Position of *contact discontinuity*

Comparing thermal and non-thermal X-ray emission, Warren et al. (2005) measured the position of CD and FS concluding that they are too close to be described by purely gaseous hydrodynamical models.

The presence of a non-negligible population of relativistic particles makes the shocked plasma more compressible and can explain this effect .

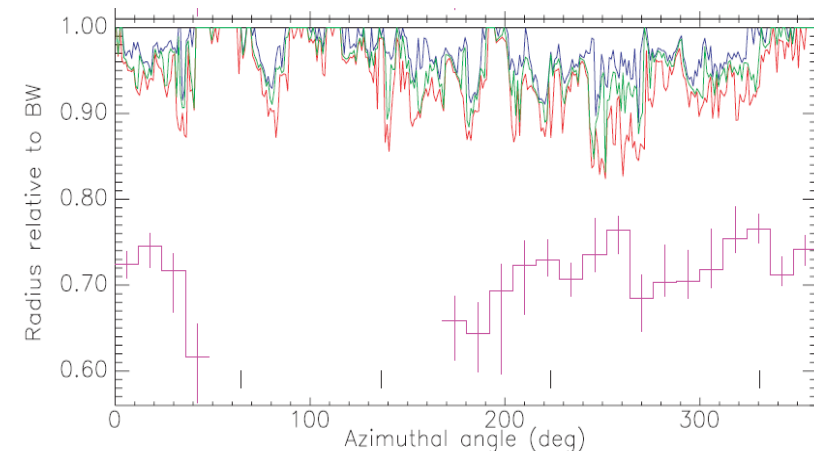
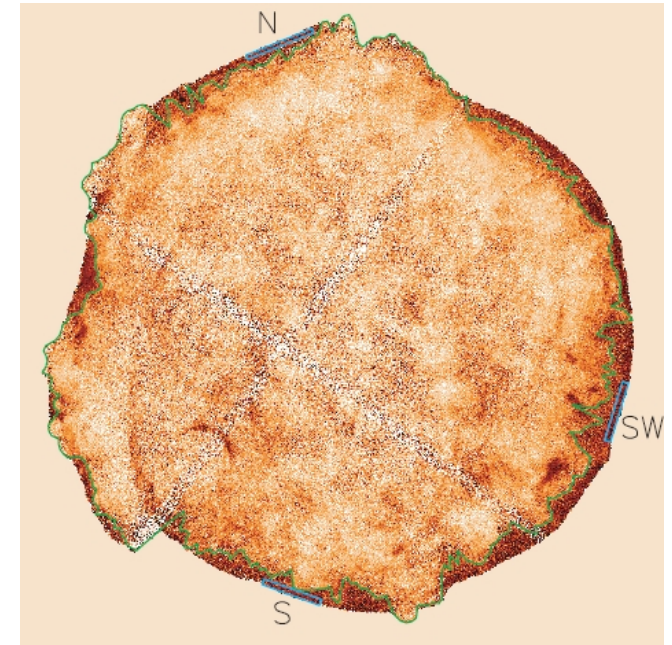
**X-ray measurement**  
(Warren et al. 2005)  $R_{CD}/R_{FS} = 0.93 \pm 2\%$

**1-D hydrodynamical simulation**  
(Wang & Chevalier 2001)  $R_{CD}/R_{FS} = 0.77 \rightarrow < 0.87$

**Our prediction**  $R_{CD}/R_{FS} = 0.87 \rightarrow \sim 0.91$

The estimated efficiency  $\sim 12\%$  well account for the CD/FS observed distance, taking into account also the effect of Raileigh-Taylor instability at the CD.

From Warren et al. (2005)



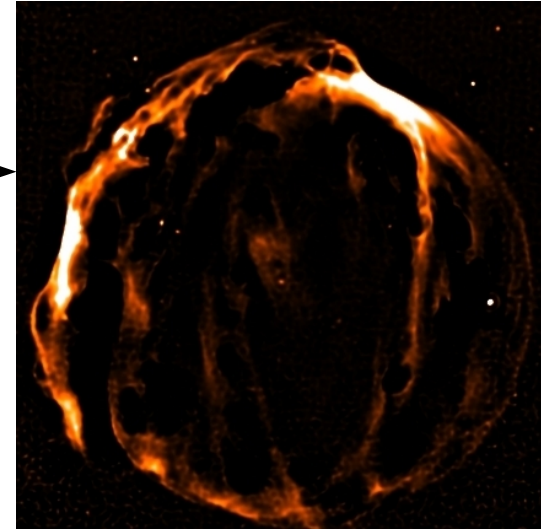
# Contribution of IR dust emission to inverse Compton scattering

IR radiation has two different component:

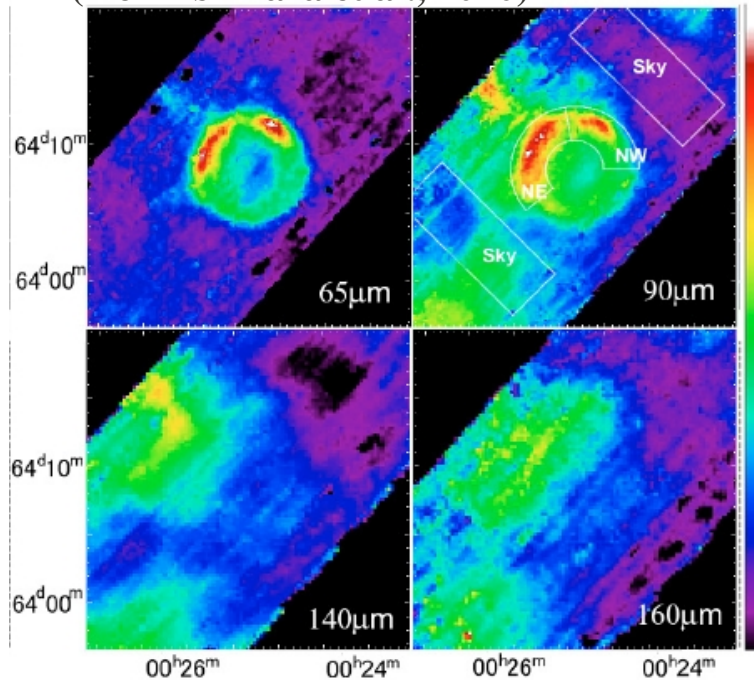
- 1) **Cold component** ( $T \sim 20$  K) correlated with the position of CO molecular cloud  $\rightarrow$  non related to the remnant
- 2) **Warm component** ( $T \sim 100$  K) due to local ISM dust heated downstream of the shock (local photon energy density  $3.1 \text{ eV/cm}^3$ )

The warm IR photons dominate the IC scattering over CMB and Galactic background light

Spitzer image at  $24 \mu\text{m}$

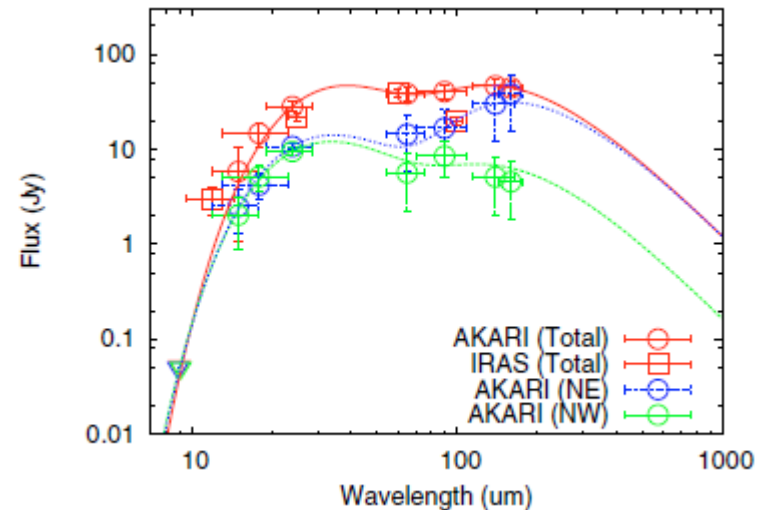


AKARI map at different wavelength  
(from Ishihara et al., 2010)



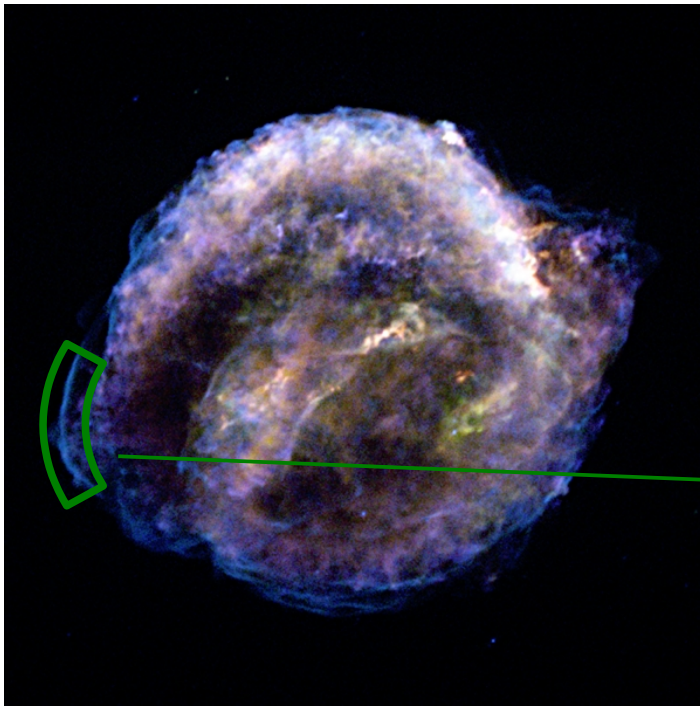
Warm  
component

Cold  
component



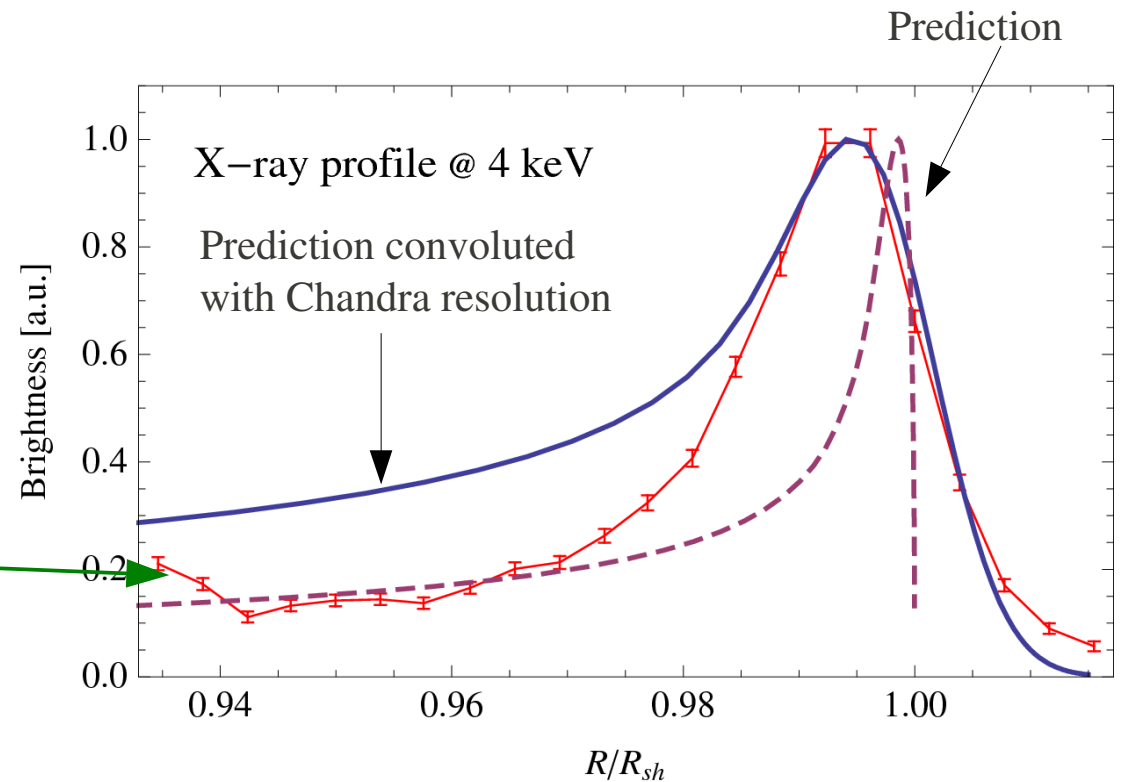
# Radial profile of X-ray emission for Kepler

- X-ray filament thickness imply  $B_2 \geq 200 \mu\text{G}$  (if interpreted as synchrotron losses).
- We find  $B_2 \approx 300 \mu\text{G}$  (the predicted thickness is smaller than the Chandra resolution).



Chandra X-ray map.

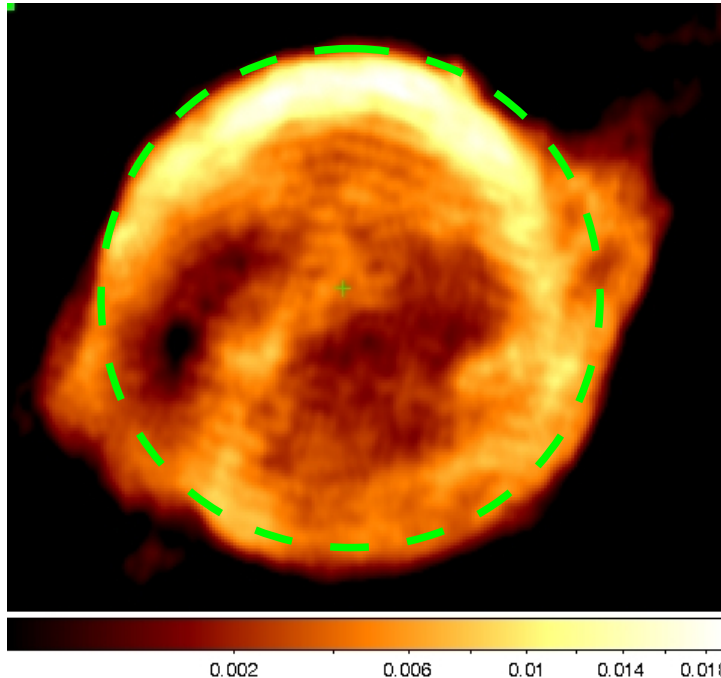
Data for the green sector are from Vink (2008)



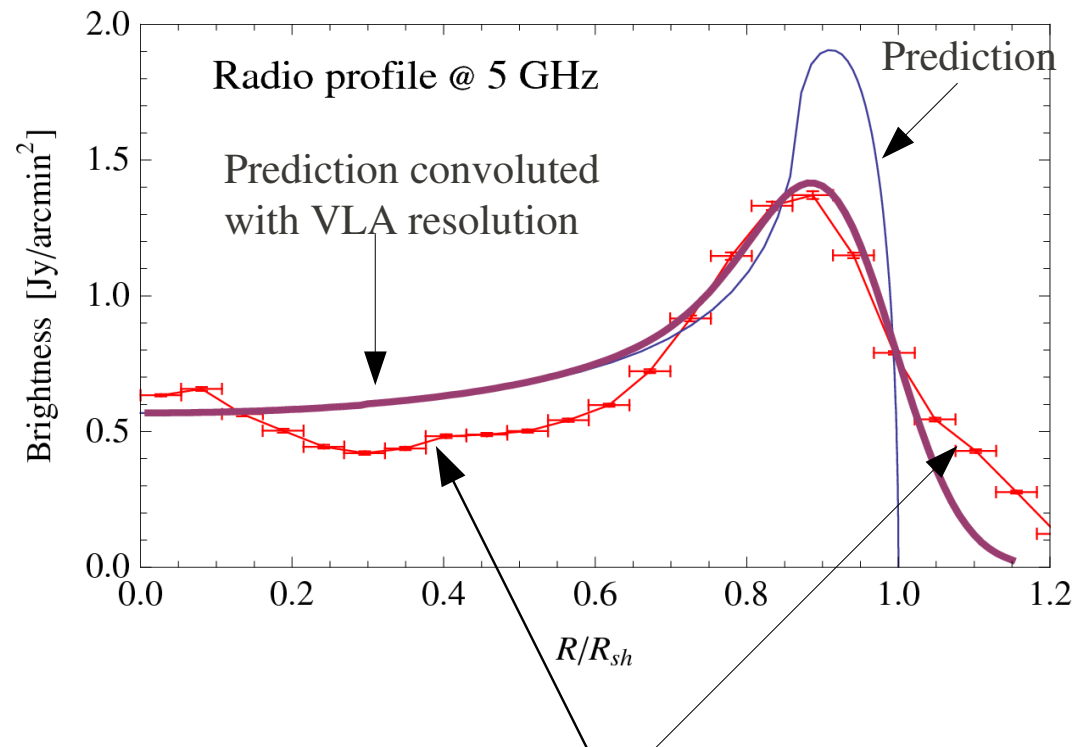


# Radial profile of radio emission for Kepler

The morphology of radio synchrotron emission is not perfectly reproduced because deviation from spherical symmetry.



Radio map at 5 GHz from  
NRAO/VLA archive Survey



These excesses could be due to deviation from spherical symmetry